Superconductivity, magnetism, and their coexistence in $R(Ni_{1-x}Co_x)_2B_2C$ (R=Lu, Tm, Er, Ho, Dy)

H. Schmidt and H. F. Braun
Physikalisches Institut, Universität Bayreuth, D-95440 Bayreuth, Germany
(Received 22 October 1996)

The effect of Co substitution on superconductivity and magnetism in the system $R(Ni_{1-x}Co_x)_2B_2C$ (R = Lu, Tm, Er, Ho, Dy) is investigated by ac-susceptibility measurements in zero and applied magnetic fields and zero-field resistivity measurements. For all R series a rapid decrease of the superconducting transition temperature T_c is observed with increasing Co substitution, while the magnetic transition temperatures show only small changes. It is observed that the initial depression rate of T_c grows in magnitude in the R series from Lu to Ho. For the nonmagnetic system $Lu(Ni_{1-x}Co_x)_2B_2C$ the mechanisms leading to the decrease in T_c are analyzed and discussed. It was found that a transition from clean to dirty limit behavior occurs with Co doping. For the magnetic systems $R(Ni_{1-x}Co_x)_2B_2C$ R = Tm, Er, where antiferromagnetism and superconductivity coexist, the influence of Co doping results in the occurrence of anomalous behavior of ac-susceptibility, resistivity and the upper critical fields when T_c comes close to the magnetic transition temperatures T_N. For $Er(Ni_{1-x}Co_x)_2B_2C$ reentrant-like behavior is observed, similar to that present in $HoNi_2B_2C$. The reentrant behavior of $HoNi_2B_2C$ is enhanced with Co doping. Possible reasons for that behavior are discussed. [S0163-1829(97)04614-6]

I. INTRODUCTION

The recent discovery of superconductivity in quaternary intermetallic RNi_2B_2C compounds (R = Y, Sc, Th, rare earths)[1–8] has attracted growing interest by several research groups. The compounds crystallize in the tetragonal $ThCr_2Si_2$ structure which can be displayed as a framework of alternating R-C and Ni_2B_2 layers.[9] Band structure calculations[10–12] reveal a three-dimensional electronic behavior in qualitative agreement with spectroscopic measurements.[13,14] The superconducting properties can be derived from a conventional strong-coupling mechanism involving B and C atoms.[15] The density of states (DOS) shows a peak at the Fermi level which is mainly composed of Ni-3d states, but with non-negligible contributions of all the other elements.[10]

Superconductivity is observed not only for the nonmagnetic rare earths, but also for the magnetic rare earths Tm, Er, Ho, and Dy.[3] The relatively high superconducting transition temperatures up to 16.6 K and the existence of magnetic order in the range 1.5 to 10 K make these systems suitable for a study of interplay between superconductivity and magnetism. For the compounds R = Tm, Er, and Dy coexistence between superconductivity and antiferromagnetism is observed. The compound $ErNi_2B_2C$ exhibits an incommensurate antiferromagnetic ground state with a modulation of the magnetic moments along the a axis (or b axis) with a wave vector $q = 0.553\ \mathbf{a}^*$ (Refs. 16 and 17), a Néel temperature T_N = 5.8 K and a superconducting transition at a higher temperature of about 10–11 K.[3,18] In contrast, the antiferromagnetic ground state of $TmNi_2B_2C$ [T_N = 1.5 K (Ref. 19)] consists of ferromagnetic (110) planes aligned along the c axis, sinusoidally modulated along the (110) direction.[20] Superconductivity appears at about 11 K.[3] $DyNi_2B_2C$ shows antiferromagnetic ordering at about 10 K, while at even lower temperatures (4 to 6 K) a transition into the superconducting state evolves.[6–8] The magnetic structure consists of ferromagnetically aligned Dy spins in the ab plane, but antiferromagnetically coupled along the c axis.[21] For the compound $HoNi_2B_2C$ reentrant behavior is observed.[3,22] This interesting behavior is probably caused by the interaction of a superconducting phase (T_c = 7–8 K), a spiral-magnetic phase modulated along the c axis ($q = 0.915\ \mathbf{c}^*$, T_M = 5.8 K) and an antiferromagnetic phase (T_N = 5 K), with the same structure as observed for $DyNi_2B_2C$.[23,24] The pair-breaking effect which causes reentrant behavior is attributed to the spiral-magnetic phase where the neighboring ferromagnetically aligned sheets of Ho spins in the basal plane are turned approximately by 160 °C along the c axis and produce a net ferromagnetic component on the Ni sheets.[23] In addition the same a-axis modulated structure as for $ErNi_2B_2C$ with a similar modulation vector $q = 0.585\ \mathbf{a}^*$ is observed.[24] This a-axis modulated structure is also observed in the nonsuperconducting compounds $TbNi_2B_2C$ (Ref. 25) and $GdNi_2B_2C$ (Ref. 26) and seems to be a common feature of the the whole series of rare-earth borocarbides, resulting from Fermi surface nesting effects.[27]

The ratio of the magnetic over the superconducting transition temperatures T_N/T_c is smaller than one for the antiferromagnetic superconductors $TmNi_2B_2C$ ($T_N/T_c \approx 0.15$) and $ErNi_2B_2C$ ($T_N/T_c \approx 0.6$), close to one for the superconductor showing reentrant behavior $HoNi_2B_2C$ ($T_M/T_c \approx 0.8$) and larger than one for $DyNi_2B_2C$ ($T_N/T_c \approx 2.4$). In this context, it is interesting to examine in which way the interplay between superconductivity and magnetism is influenced when T_M/T_c is changed by substitution. To obtain information about this, we carried out a study of the systems $R(Ni_{1-x}Co_x)_2B_2C$ for R = Lu, Tm, Er, Ho, Dy in the range $0 \leqslant x \leqslant 0.2$. The choice of Co as dopant for Ni is based on the fact that T_c decreases rapidly when Ni

is partially replaced by Co as shown for the system $Y(Ni_{1-x}Co_x)_2B_2C$,[28] that the sublattice of R ions remains undisturbed with doping, and that complete solid solutions can be formed in the investigated concentration range.

II. EXPERIMENTAL

The samples were prepared from the elements by arc melting amounts of R (99.9%), Ni (99.9%), B (99%), and C (99.5%) under argon atmosphere. First, alloys with composition RNi_2B_2C and $R(Ni_{0.8}Co_{0.2})_2B_2C$ were melted and annealed 4 days at 1100 °C under argon to obtain homogeneous samples as starting material. From these alloys the final samples were produced by arc melting. After that a further heat treatment of 4 days at 1100 °C was carried out. All samples were characterized by x-ray powder patterns taken on a powder diffractometer with secondary monochromator (CuK_α radiation). The lattice parameters were refined with the method of least squares using Si as internal standard. For characterization of the superconducting and magnetic properties the samples were investigated with an ac inductive technique at a frequency $f = 18$–28 Hz and an ac-amplitude $H_{ac} = 1$ Oe in zero and applied magnetic dc field up to 9 T in the range 1.2 to 20 K. Resistivity measurements were done by an ac four-probe technique at 28 Hz with current densities between $j = 0.5$ and 18 A/cm^2.

III. RESULTS AND DISCUSSION

A. X-ray diffractometry

From an analysis of the x-ray diffraction powder patterns the amount of impurity phases present in a sample can be assessed. All samples series were single phase, or almost single phase, with a maximum amount of impurity phases of about 1%. An investigation of the system $Y(Ni_{1-x}Co_x)_2B_2C$ (Ref. 28) shows that solid solubility includes at least the concentration range $0 \leqslant x \leqslant 0.9$. A metallographic study carried out on the undoped sample $HoNi_2B_2C$ and the sample $Ho(Ni_{0.8}Co_{0.2})_2B_2C$ reveal anisometric grains of the size 100–300 μm$\times$50–80 μm and the existence of minor amounts of impurity phase located at the grain boundaries, which is the same for both samples. No evidence for Co-rich segregations can be found. We conclude that complete solid solutions of RNi_2B_2C and RCo_2B_2C are formed in the concentration range $0 \leqslant x \leqslant 0.2$ for R = Lu, Tm, Er, Ho, and Dy.

The dependence of the lattice parameters a, c, and the volume of the unit cell V on Co concentration is given in Table I. The c axis shows a linear decrease for all compounds ranging from 2.9 to 5.6×10^{-3} Å/at. %. The a-axis parameter is almost constant for the Lu- and Tm-system while a very small linear decrease is seen for the rest of the compounds, which is about one order of magnitude smaller than for the c axis. No clear correlation of the change of lattice parameters with the rare earth is observed. The change of the volume of the unit cell is also very small in the concentration range observed, lower than 0.5% for all compounds. This is consistent with a continuous incorporation of Co on Ni sites without significant change of the atomic distances.

TABLE I. Dependence of lattice parameters a, c, and volume of the unit cell V on Co concentration for $R(Ni_{1-x}Co_x)_2B_2C$ (R = Lu, Tm, Er, Ho, Dy).

R	da/dx 10^{-3} Å/at. %	dc/dx 10^{-3} Å/at. %	dV/dx Å^3/at. %
Lu	0.05(8)	−4.9(2)	−0.057(9)
Tm	0.04(9)	−4.5(3)	−0.048(5)
Er	−0.26(5)	−5.6(2)	−0.089(5)
Ho	−0.15(5)	−3.4(2)	−0.053(2)
Dy	−0.59(8)	−2.9(2)	−0.075(8)

B. ac-susceptibility and resistivity measurements

In Fig. 1 the superconducting transition temperatures T_c for all the compounds $R(Ni_{1-x}Co_x)_2B_2C$ (R = Lu, Tm, Er, Ho, Dy) are plotted in the range $0 \leqslant x \leqslant 0.2$. T_c was taken at the onset of the superconducting transition which is defined at 10 % of the full signal change of the real part of the ac susceptibility. For all compounds a decrease in T_c is observed with increasing incorporation of Co on Ni sites. The properties of the individual systems are discussed in the following sections.

1. The system $Lu(Ni_{1-x}Co_x)_2B_2C$

For low Co concentrations, T_c of $Lu(Ni_{1-x}Co_x)_2B_2C$ starts to drop linearly, but exhibits a positive curvature and a tendency to saturate for higher Co content. The overall behavior is very similar to the curve observed for $Y(Ni_{1-x}Co_x)_2B_2C$, which was investigated by several authors.[28–30] In comparison to the systems containing magnetic rare earths, $Lu(Ni_{1-x}Co_x)_2B_2C$ can be seen as a nonmagnetic reference system, where the mechanisms leading to a decrease in T_c can be analyzed.

For a closer inspection of the system we have determined the upper critical fields H_{c2} of $Lu(Ni_{1-x}Co_x)_2B_2C$ for four samples with different Co content, $x = 0.0$, 0.03, 0.09, and 0.15, which are plotted on an absolute [Fig. 2(a)] and a rela-

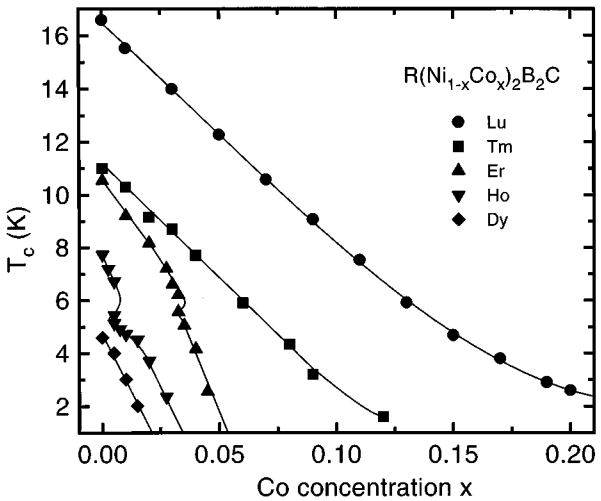

FIG. 1. Dependence of the superconducting transition temperature T_c on Co concentration for the compounds $R(Ni_{1-x}Co_x)_2B_2C$ (R=Lu, Tm, Er, Ho, and Dy).

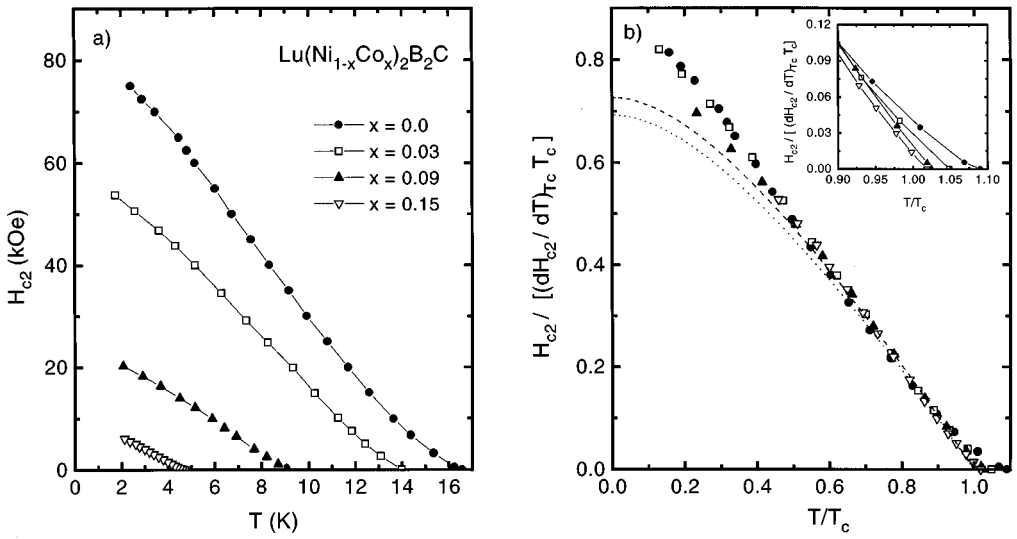

FIG. 2. Upper critical fields of $Lu(Ni_{1-x}Co_x)_2B_2C$ for $x = 0.0, 0.03, 0.09, 0.15$ plotted in applied (a) and reduced variables (b); the theoretical curves according to WHH theory (Ref. 36) are plotted for the clean (dashed line) and dirty (dotted line) limit.

tive [Fig. 2(b)] scale. No anomalous temperature dependence of H_{c2} is observed which would be expected if Co doping introduces magnetic impurity moments. This indicates that Co loses its magnetic moment in the structure and we deal with doping by nonmagnetic impurities. This assumption was also justified by superconducting quantum interference device measurements on $Y(Ni_{1-x}Co_x)_2B_2C$.[28]

A factor which might influence T_c is chemical pressure effects, caused by the compression of the volume of the unit cell observed with Co doping (Table I). This effect can be assessed with the relation

$$\Delta T_c = \Delta V \frac{dT_c}{dp}\frac{B}{V}. \tag{1}$$

B is the bulk modulus which was determined to 1.2×10^3 kbar for YNi_2B_2C.[31] The pressure coefficient dT_c/dp for the borocarbide compounds ranges from -0.06 to 0.02 K/kbar (Refs. 22 and 40) and the maximum volume change ΔV for the relevant Co concentration range is about 0.4 $Å^3$. This should result in a maximum T_c change of -0.2 to 0.08 K indicating that pressure effects are of minor importance.

Thus the main reason for the decrease in T_c has to be looked for in a change of the electronic or phononic properties of the compounds. Since the lattice parameters show only a small change of $\Delta a/a \leqslant 0.1\%$ and $\Delta c/c \leqslant 0.3\%$ for the different rare-earth compounds in the concentration range where T_c decreases, we can assume the simple model of rigid bands and a phonon spectrum remaining unchanged with Co doping. Due to the peak in the density of states (DOS) at the Fermi level $N(E_F)$, the decrease in T_c should be caused by a decrease in $N(E_F)$ due to hole doping with increasing Co concentration. Hoellwarth *et al.* showed by specific-heat measurements on $Y(Ni_{1-x}Co_x)_2B_2C$ that the decrease in T_c can indeed be correlated to a decrease in $N(E_F)$ consistent with the above assumptions.[32]

For the evaluation of the electron-phonon interaction parameter λ with increasing Co content it is possible to use the Allen and Dynes equation[33]

$$T_c = F\exp\left(-\frac{1.04(1+\lambda)}{\lambda-\mu^*-0.62\lambda\mu^*}\right). \tag{2}$$

F is a prefactor given by

$$F = \frac{\omega_{ln}}{1.20}\left[1+\left(\frac{\lambda}{2.46(1+3.8\mu^*)}\right)^{3/2}\right]^{1/3} \times\left[1+\frac{[(\omega_2/\omega_{ln})-1]\lambda^2}{\lambda^2+1.82(1+6.3\mu^*)(\omega_2/\omega_{ln})}\right]. \tag{3}$$

ω_n is the nth generalized moment of the electron-phonon spectral function $\alpha^2(\omega)F(\omega)$ resulting from Eliashberg theory. H. Michor *et al.*[34] have constructed a model phonon spectrum from normal-state specific-heat data of $LuNi_2B_2C$ and determined the generalized moments to $\omega_1 = 232$ K, $\omega_2 = 311$ K, and $\omega_{ln} = 173$ K for $\alpha^2 \sim \omega^{-0.5}$. With the help of these results and assuming a Coulomb pseudopotential of $\mu^* = 0.13$ the electron-phonon enhancement factor λ can be derived. A decrease of λ from 1.15 for $LuNi_2B_2C$ to 0.67 for $Lu(Ni_{0.85}Co_{0.15})_2B_2C$ is obtained from the decrease of T_c as given in Table II. Assuming a linear dependence of λ with $N(E_F)$:

$$\lambda = \frac{N(E_F)V^*}{M\omega_2^2}, \tag{4}$$

where V^* is the electron-phonon matrix element and M is the molar mass, we derive a reduction of $N(E_F)$ of about 40% in the investigated composition range. This is in qualitative agreement with the reduction of $N(E_F)$ determined by specific-heat experiments on $Y(Ni_{1-x}Co_x)_2B_2C$ samples.[32]

For a more detailed discussion of the upper critical fields for $Lu(Ni_{1-x}Co_x)_2B_2C$ the $H_{c2}(T)$ curves are plotted in reduced variables [Fig. 2(b)]. The overall behavior for the samples is not very different. In the low field range the undoped sample $LuNi_2B_2C$ exhibits a significant positive deviation of H_{c2} from the expected linear dependence near T_c, which is consistent with resistivity and specific-heat

TABLE II. Some important superconducting and normal-state parameters of $Lu(Ni_{1-x}Co_x)_2B_2C$, $x=0$, 0.03, 0.09, and 0.15.

Compound	$T_{c,on}$ (K)	λ	$(dH_{c2}/dT)_{Tc}$ (kOe/K)	ρ_0 ($\mu\Omega$ cm)	l_{tr} (nm)	ξ_0 (nm)	ξ_0/l_{tr}
$LuNi_2B_2C$	16.6	1.15	5.59±4	6±1	11	10	0.9
$Lu(Ni_{0.97}Co_{0.03})_2B_2C$	14.0	1.03	4.89±6	27±4	2.4	26	11
$Lu(Ni_{0.91}Co_{0.09})_2B_2C$	8.8	0.85	3.27±4	62±9	1.1	100	91
$Lu(Ni_{0.85}Co_{0.15})_2B_2C$	4.8	0.67	2.47±2	94±14	0.7	343	490

measurements given in literature.[3,34] This deviation becomes less pronounced for the Co-doped samples as can be seen in the inset of Fig. 2(b). For an estimate of the value $(dH_{c2}/dT)_{Tc}$, the linear part of $H_{c2}(T)$ is extrapolated to zero and chosen as initial linear increase. The experimental $(dH_{c2}/dT)_{Tc}$ values are shown in Table II. It is clearly visible that $(dH_{c2}/dT)_{Tc}$ shows a nonlinear decrease with growing Co content from 5.6 to 2.5 kOe/K.

Based on specific-heat measurements of $LuNi_2B_2C$ (Ref. 34) and the measurements presented here, a crude estimation of the electron mean free path l_{tr} and the coherence length ξ_0 can be made. l_{tr} can be determined according to the relation[35]

$$l_{tr}=\frac{3}{\rho_0 N(E_F) v_F e^2}\approx\frac{3\pi h}{e^2\rho_0 S}, \tag{5}$$

where ρ_0 is the residual resistivity, v_F the Fermi velocity, and S the Fermi surface area. ρ_0 was determined by resistivity measurements on bulk samples with a defined geometry and is given in Table II. Using $N(E_F)$ = 4.8 states $(\text{eV cell})^{-1}$ and $v_F=3.6\times10^7$ cm/s obtained from band structure calculations[11] we can compute the mean-free path for $LuNi_2B_2C$. For the calculation of l_{tr} for the Co-doped samples we assume that the Fermi surface area S does not change significantly with Co doping and $l_{tr}\sim1/\rho_0$. We obtain a strong decrease of l_{tr} from 11.0 to 0.7 nm with increasing incorporation of Co as additional scattering centers.

ξ_0 can be obtained from the equation[35]

$$-\frac{\phi_0}{2\pi}\frac{1}{(H_{c2}/dT)_{T_c}T_c}=0.546\left[\frac{1}{\xi_o^2}+0.882\frac{1}{\xi_0 l_{tr}}\right]^{-1}R\left(\frac{\xi_0}{l_{tr}}\right), \tag{6}$$

where Φ_0 is the flux quantum and $R(\xi_0/l_{tr})$ is a function of the order of unity which can be neglected for our purposes. From Table II it is seen that ξ_0 increases from 10 to 343 nm with Co doping. The ratio ξ_0/l_{tr} which ranges from 0.9 for $LuNi_2B_2C$ to 490 for $Lu(Ni_{1.85}Co_{0.15})_2B_2C$ indicates that the system seems to be close to the clean limit for the undoped sample. A transition to the dirty limit results from doping with Co. It should be noted that the derived absolute values for ρ_0, and thus for ξ_0/l_{tr}, have to be seen as an upper limit, since the intrinsic values might be lower due to the porosity of the samples. Since all samples were prepared in the same way, the relative increase of ρ_0 with Co doping describes the essential physical behavior.

In Fig. 2(b), the reduced critical field curves are compared to the theoretical curves for weak electron-phonon coupling obtained by Helfand and Werthamer for the clean and dirty limits.[36] The theoretical clean limit curve is very similar to the one obtained for the dirty limit but results in a 6% higher $H_{c2}(0)$. A difference of that order is also seen for upper critical fields of the undoped sample $LuNi_2B_2C$ in comparison to the Co-rich sample $Lu(Ni_{0.91}Co_{0.09})_2B_2C$ near $T=0$. This behavior can be explained with the transition from clean to dirty limit derived from the low field data.

A more striking feature is the fact that the theoretical fits underestimate $H_{c2}(0)$ by about 15% independent of the degree of Co doping. Possible reasons for this behavior might be found in strong-coupling effects or anisotropy and multiband effects. According to the specific-heat data and the derived model phonon spectrum for $LuNi_2B_2C$ (Ref. 34) strong-coupling effects are not able to explain this enhancement. Therefore we attribute the difference between theory and experiment to combined effects of the anisotropy of the Fermi surface and the fact that several bands with different Fermi velocities and scattering times contribute to the DOS at the Fermi level.[10] As pointed out in Ref. 37 such effects can enhance the upper critical fields by about 20–30 %.

2. Depression of T_c in the paramagnetic range

As can be seen in Fig. 1, the magnetic compounds show also a linear depression of T_c with Co substitution in the paramagnetic range as was observed for the nonmagnetic compounds. For higher Co doping, deviations become visible as anomalies around the magnetic transition temperatures. For $Dy(Ni_{1-x}Co_x)_2B_2C$, where superconductivity evolves in the presence of antiferromagnetism for all samples, the behavior is nearly linear in the measured concentration range. For a further analysis it is interesting to compare the depression of T_c with increasing Co content for the different rare-earth compounds. The value of dT_c/dx (Table III) is not constant for different rare earths, but grows in magnitude from −2.5 K/at. % for the Lu system to −6.1 K/at. % for the Ho system. The value for

TABLE III. Initial linear decrease of T_c with Co content.

Compound	$T_{c,on}$ (K)	dT_c/dx K/at. %
$Lu(Ni_{1-x}Co_x)_2B_2C$	16.6	− 2.5(1)
$Tm(Ni_{1-x}Co_x)_2B_2C$	11.0	−2.6(1)
$Er(Ni_{1-x}Co_x)_2B_2C$	10.5	−3.6(1)
$Ho(Ni_{1-x}Co_x)_2B_2C$	7.7	−6.1(2)
$Dy(Ni_{1-x}Co_x)_2B_2C$	4.7	−5.2(4)

$Dy(Ni_{1-x}Co_x)_2B_2C$ cannot be compared with the other values, since the antiferromagnetic state is stable for all samples.

In searching for an explanation for that behavior we should keep in mind that for the undoped RNi_2B_2C compounds T_c is depressed due to magnetic pair breaking when the nonmagnetic Lu is replaced by magnetic rare earths. This decrease in T_c scales roughly with the de Gennes factor $G=(g_{J-1})^2J(J+1)$:[3]

$$\Delta T_c = -\frac{\pi^2}{2k_B} cN(E_F)I^2G, \tag{7}$$

where $c = 1/6$ is the concentration of magnetic moments and I the exchange constant. We expect that this R-dependent depression rate should be decreased due to the decrease in $N(E_F)$ when Ni is partially replaced by Co. As a consequence, the Co-dependent depression rate dT_c/dx should decrease with increasing G and not increase as observed.

To explain our measurements we could assume an effective exchange coupling constant I_{eff} which increases with Co concentration x. This would result in increased magnetic pair breaking for samples with higher Co content and in a Co-dependent depression rate dT_c/dx which increases with G. W. Weber has speculated that a complex order parameter exists in the paramagnetic phase which suppresses the R $5d$ contributions to the superconducting wave function by destructive interference. This complex order parameter (possibly of extended s type) should be very sensitive to disorder effects, resulting in a rapid decrease of T_c with doping on the Ni or B sublattice.[38] Also, point contact spectroscopy data on $HoNi_2B_2C$ by Rybaltchenko *et al.* has been interpreted as indicating two different superconducting phases, one for the paramagnetic region which is of unknown type, and a BCS-type phase in the antiferromagnetic ordered state.[39]

3. Interplay between superconductivity and magnetism in $R(Ni_{1-x}Co_x)_2B_2C$ (R =Ho,Er,Tm)

When the nonmagnetic Lu in the compound $LuNi_2B_2C$ is replaced by a magnetic rare earth, magnetic order occurs and interplay between superconductivity and magnetism is observed. In this section we examine how the interplay between magnetic order and superconductivity is modified when Ni is partially replaced by Co and especially what happens when the superconducting transition temperature T_c comes close to, or crosses the magnetic ordering temperatures.

In Fig. 3 the real part of the ac susceptibility is plotted for $Ho(Ni_{1-x}Co_x)_2B_2C$ in a concentration range from $x=0$ to $x=0.035$ corresponding to the substitution of 0 to 3.5 % Co for Ni. As can be seen, only partial reentrant behavior is established for the undoped sample $HoNi_2B_2C$ with a superconducting onset of 7.7 K and a reentrant maximum of about 25% of the normal-state value around T_N = 5.3 K. With increasing Co doping, T_c is lowered and the reentrant peak increases resulting in a fully reentrant sample which reaches the normal state at T_N ($x=0.005$). Further increase of the Co concentration leads to the vanishing of reentrant behavior ($x>0.0075$), the magnetic transitions are manifested as a broad maximum and the superconducting state evolves in presence of an antiferromagnetically ordered sublattice of

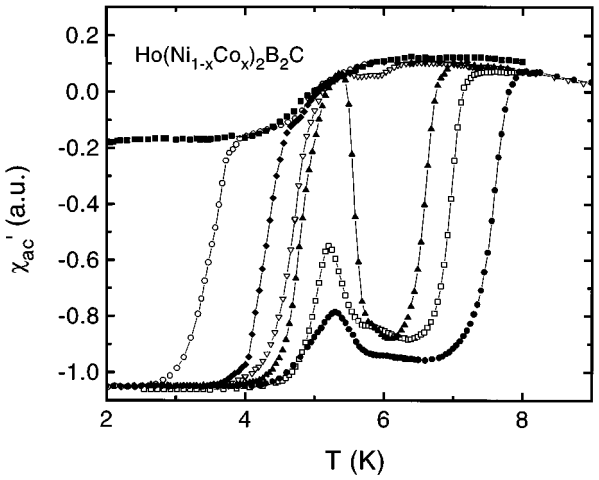

FIG. 3. Temperature dependence of the real part of ac susceptibility for $Ho(Ni_{1-x}Co_x)_2B_2C$; closed circle: $x=0.0$, open square: $x=0.003$, closed uptriangle: $x=0.005$, open downtriangle: $x=0.0075$, closed diamond: $x=0.015$, open circle: $x=0.02$, closed square: $x=0.035$.

R ions ($x=0.02$). The behavior of this sample is qualitatively the same as observed for $DyNi_2B_2C$.[6–8] An increase of the Co content above about 3% leads to the complete depression of superconductivity in the temperature range measured and we obtain a nonsuperconducting magnetic sample as also observed by composition dependent studies in the homogeneity range of $HoNi_2B_2C$.[40,41]

For a more detailed study, three samples of the systems $Ho(Ni_{1-x}Co_x)_2B_2C$, with $x=0$, 0.005, and 0.015 were investigated in an applied magnetic dc field. The upper critical fields H_{c2} are plotted in Fig. 4. The undoped compound $HoNi_2B_2C$ shows the typical nonmonotonic behavior with a maximum at 6.3 K and a 350-Oe deep minimum around T_N at 5.3 K, comparable to the data reported in literature.[3,41] For $Ho(Ni_{0.995}Co_{0.005})_2B_2C$, H_{c2} is depressed to zero between 5.5 and 5.1 K, which reflects the fact that this sample is fully reentrant at 5.3 K. The upper critical field of $Ho(Ni_{0.985}Co_{0.015})_2B_2C$, where $T_c<T_N$, shows conventional

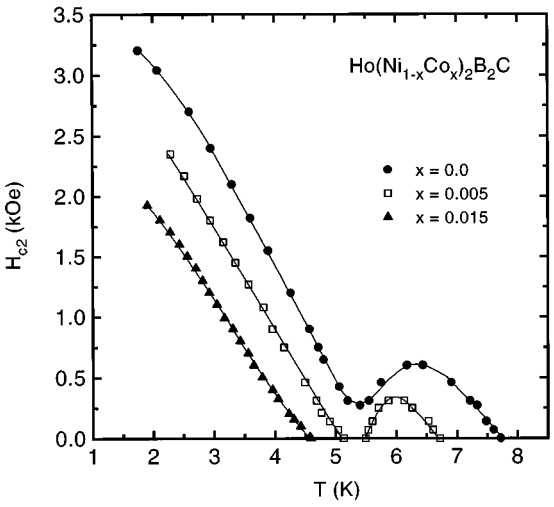

FIG. 4. Upper critical fields H_{c2} of $Ho(Ni_{1-x}Co_x)_2B_2C$ for x = 0.0, 0.005, 0.015.

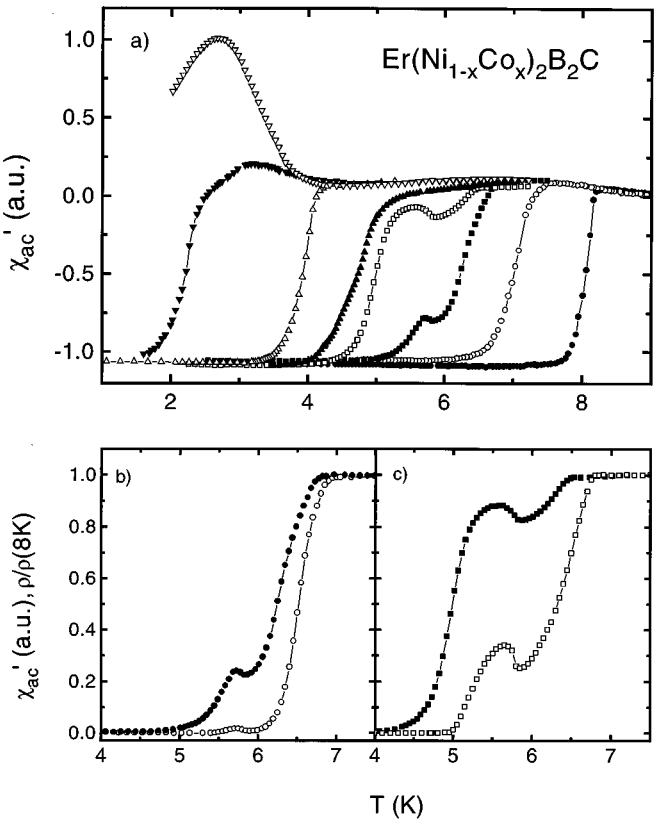

FIG. 5. (a) Temperature dependence of the real part of ac susceptibility for $Er(Ni_{1-x}Co_x)_2B_2C$; closed circle: $x=0.02$, open circle: $x=0.0275$, closed square: $x=0.03$, open square: $x=0.0325$, closed uptriangle: $x=0.035$, open uptriangle: $x=0.0375$, closed downtriangle: $x=0.045$, open downtriangle: $x=0.055$. Comparison of resistivity for $j = 3$ A/cm^2 (open symbols) and ac susceptibility (closed symbols) for (b) $Er(Ni_{0.97}Co_{0.03})_2B_2C$ and (c) $Er(Ni_{0.9675}Co_{0.0325})_2B_2C$.

behavior over the whole measured temperature range without any anomalies, qualitatively similar to the H_{c2} curve of $DyNi_2B_2C$.[8]

For the $Er(Ni_{1-x}Co_x)_2B_2C$ system the ac susceptibility data are plotted in Fig. 5(a). For $x<0.03$ a conventional superconducting transition is seen like in the undoped compound $ErNi_2B_2C$, which is lowered with increasing Co content. When T_c comes close to the magnetic transition temperature $T_N \approx 5.8$ K anomalies in the ac-susceptibility become visible for the samples with composition $x=0.03$ and $x=0.0325$. For higher Co content a conventional superconducting transition is observed again, until superconductivity disappears and a positive ac-susceptibility signal is seen which we attribute to an additional magnetic transition.

In Figs. 5(b) and 5(c), the data for two samples which exhibit anomalies in the ac susceptibility are plotted in an expanded scale together with the normalized resistivity. $Er(Ni_{0.97}Co_{0.03})_2B_2C$ clearly shows a maximum in both ac susceptibility and resistivity at 5.75 K. The maximum is less pronounced in resistivity and zero resistivity is reached above the maximum at about 6 K. It has to be mentioned that the size of the maximum in resistivity depends weakly on the applied transport current, a behavior which is also observed for the reentrant maximum of $HoNi_2B_2C$.[42] For

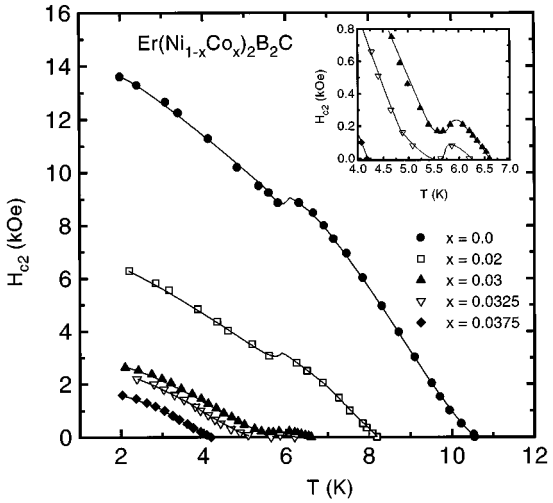

FIG. 6. Upper critical fields H_{c2} of $Er(Ni_{1-x}Co_x)_2B_2C$ for $x = 0.0, 0.02, 0.03, 0.0325, 0.0375$.

$Er(Ni_{0.9675}Co_{0.0325})_2B_2C$ there exist well visible maxima for ac-susceptibility and resistivity data at 5.65 K. In this sample the upper superconducting transition is strongly suppressed and zero resistivity is not reached above the maximum. It is obvious that the ac-susceptibility and resistivity data of these samples show similarity to the reentrant behavior observed for the undoped $HoNi_2B_2C$ sample (Fig. 3). It should be noted that the effect of creating reentrantlike behavior by bringing T_c close to T_N does not depend on the choice of Co as dopant to lower T_c, since experiments for the system $Er(Ni_{1-x}Fe_x)_2B_2C$ reveal the same behavior.[42]

The upper critical fields of the $Er(Ni_{1-x}Co_x)_2B_2C$ system are displayed in Fig. 6. For $ErNi_2B_2C$ the behavior of H_{c2} is as expected for superconductors with a regular lattice of magnetic ions showing a magnetic phase transition below T_c. The influence of the antiferromagnetic transition at 5.8 K is seen as a small dip in the $H_{c2}(T)$ curve in agreement with the curves extracted from resistivity measurements performed by Eisaki *et al.*[3] For the Co-doped samples the dip is nearly unchanged in shape and temperature as seen for the sample with $x=0.02$. When T_c comes close to T_N ($x=0.03$ and $x=0.0325$) the reentrantlike behavior seen in the zero-field ac-susceptibility and resistivity measurements is also reflected in H_{c2} in the form of a 90-Oe deep minimum, which dips to the zero-field axis below T_c for $Er(Ni_{0.9675}Co_{0.0325})_2B_2C$ (see inset of Fig. 6). The upper critical field of $Er(Ni_{0.9625}Co_{0.0375})_2B_2C$, where T_c is below T_N, shows no anomalies and can be compared to H_{c2} of $DyNi_2B_2C$ and $Ho(Ni_{0.985}Co_{0.015})_2B_2C$.

For the system $Tm(Ni_{1-x}Co_x)_2B_2C$ coexistence between superconductivity and magnetism is observed for Co concentrations up to 12% [Fig. 7(a)]. The sample with composition $Tm(Ni_{0.88}Co_{0.12})_2B_2C$ exhibits the onset of a superconducting transition in ac susceptibility at 1.65 K, but does not reach full shielding. The susceptibility starts to rise to the normal state value again in the vicinity of the antiferromagnetic transition at 1.5 K. The resistivity of the sample does not show a clear visible anomaly, but reaches zero resistivity only for very low current densities. With increasing transport current, zero resistivity is no longer reached, resulting in a

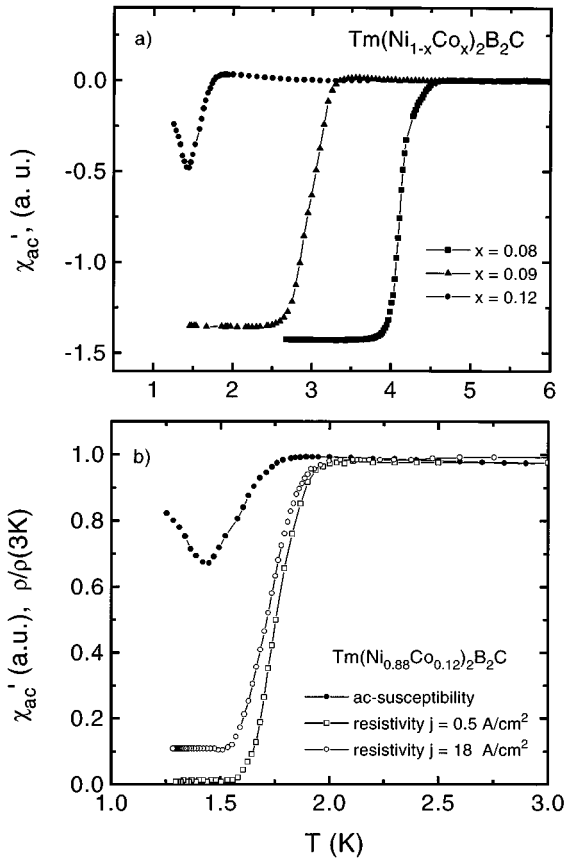

FIG. 7. (a) Temperature dependence of the real part of ac susceptibility for $Tm(Ni_{1-x}Co_x)_2B_2C$ for $x = 0.08, 0.09, 0.12$; (b) ac susceptibility and resistivity for $Tm(Ni_{0.88}Co_{0.12})_2B_2C$ for different current densities.

resistivity drop of only 88% for $j=18$ A/cm^2. Such a behavior illustrates the fact that the effect of magnetic transitions on superconductivity is also visible in resistivity. Further interpretation of these results and a comparison to the Er system is not possible due to the fact that the attainable temperature range for measurements is limited to 1.2 K by the experimental setup.

For $Ho(Ni_{1-x}Co_x)_2B_2C$ (Fig. 8) and $Er(Ni_{1-x}Co_x)_2B_2C$ (Fig. 9) the low-temperature phase diagrams are constructed for low Co concentrations. The magnetic ordering temperatures are taken from the maxima of the ac susceptibility in zero and applied magnetic fields. For the low-temperature phase diagram of the Ho system, T_c decreases rapidly, but the spiral-magnetic transition temperature T_M and the antiferromagnetic transition temperature T_N are only slightly modified. For $x<0.0075$ reentrant behavior is present which is enhanced with increasing x, seen as an anomalous deviation of the T_c curve. In the range $0.0075<x<0.038$ coexistence of antiferromagnetism and superconductivity is observed with $T_c<T_N$. At higher Co concentrations, superconductivity is suppressed and the samples show only magnetic ordering. In the system $Er(Ni_{1-x}Co_x)_2B_2C$ there is also seen a rapid decrease of T_c while T_N stays roughly constant. The occurrence of reentrantlike behavior in a small concentration range between $0.03<x<0.034$ is seen as an anomaly when the T_c curve crosses the curve of T_N. The system exhibits coexistence of superconductivity and antiferromagnetism for $x<0.03$ with $T_c>T_N$ and for $x>0.034$ with $T_c<T_N$. For Co concentrations higher than $x=0.045$ superconductivity disappears and a further magnetic transition becomes present at about 2.2 K. This magnetic phase might be associated with possible coexistence of weak ferromagnetism and superconductivity recently reported by Canfield *et al.* for $ErNi_2B_2C$ at temperatures below 2.3 K.[43]

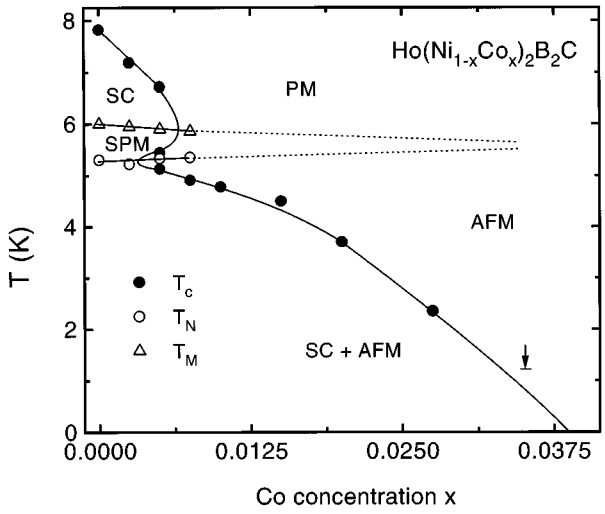

FIG. 8. Phase diagram for the system $Ho(Ni_{1-x}Co_x)_2B_2C$ for low Co concentrations; SC: superconducting, PM: paramagnetic, SPM: spiral-magnetic, AFM: antiferromagnetic.

For all magnetic systems investigated the effect of the Co substitution is to lower the superconducting transition temperature T_c, while the magnetic transition temperatures are nearly unchanged. With increasing ratio T_N/T_c the reentrant behavior of the Ho system is enhanced. We observe the occurrence of reentrantlike behavior in the Er system and anomalous behavior in the Tm system, when T_N/T_c comes close to 1.

We now discuss two possible mechanisms which might be responsible for this behavior. An explanation for our data might be that with increasing Co-doping magnetic pair

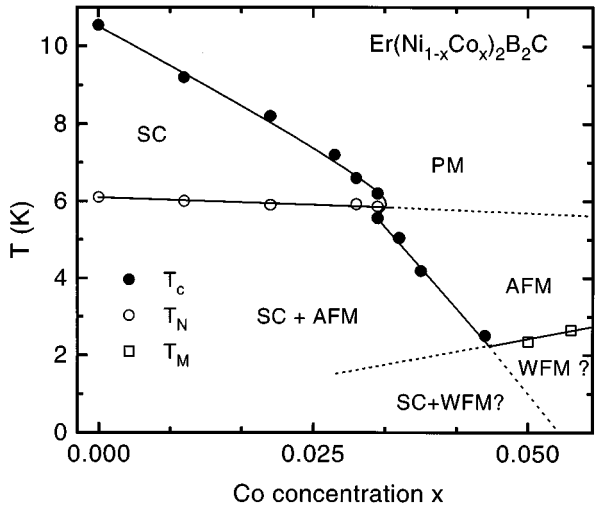

FIG. 9. Phase diagram for the system $Er(Ni_{1-x}Co_x)_2B_2C$ for low Co concentrations; SC: superconducting, PM: paramagnetic, AFM: antiferromagnetic, WFM: weak ferromagnetic.

breaking, due to magnetic ordering, is increased. This might be realized by a modification of the spiral-magnetic structure or a change of the amount of domains showing the spiral-magnetic state in the case of $Ho(Ni_{1-x}Co_x)_2B_2C$. For $Er(Ni_{1-x}Co_x)_2B_2C$, as a result of the competing ordering phenomena magnetism and superconductivity, the system could be forced to create a spiral-magnetic, or similar state, like in $HoNi_2B_2C$.

Neutron diffraction measurements on Co-doped samples of the Ho-system where performed by two different groups.[44,45] Both groups have shown that the **k** vectors of magnetic ordering are essentially the same for samples doped with different amounts of Co and undoped samples, such that a modification of the magnetic structures is unlikely. Lynn *et al.*[44] demonstrated that there exist small differences in the neutron peak intensities in both investigated systems, so that an increase of the phase fraction showing spiral-magnetic ordering and thus increased pair breaking cannot be excluded for the Ho system. For a Co-doped sample of the Er system ($T_c < T_N$) Gasser *et al.*[45] found **k** vectors of magnetic ordering changed from those of the undoped samples, with a component of **k** along c^*. A detailed study of neutron diffractometry on several samples of $Er(Ni_{1-x}Co_x)_2B_2C$ might clarify, whether the occurrence of the modified magnetic structure with Co doping is correlated with the occurrence of reentrantlike behavior.

A second mechanism which might influence the observed behavior is that we assume an unchanged pair-breaking property of the magnetic state due to nearly unchanged magnetic structures. As a consequence a decreased stability of the superconducting state should develop at T_N. A quantity which can be used to describe the stability of the superconducting state is the superconducting gap Δ. In the BCS case the temperature dependence of Δ close to T_c is given by

$$\frac{\Delta(T)}{\Delta(0)} = 1.74\left(1 - \frac{T}{T_c}\right)^{1/2}. \tag{8}$$

According to this relation a smaller gap and superconducting state less stable against magnetic pair breaking is present at T_N, when the ratio T_N/T_c approaches 1. As a consequence the increasing magnetic order parameter at T_N might be considered to cause the observed behavior.

From the results reported above it is worth to raise the question whether the reentrant behavior of $HoNi_2B_2C$ really originates from the spiral-magnetic structure, or whether it is a result of the fact that for this system T_c is close to the magnetic transition temperature(s). In this case the presence of the spiral-magnetic state would be only an additional factor contributing to a more pronounced reentrant behavior.

IV. SUMMARY

In conclusion we used resistivity and ac-susceptibility measurements in zero and applied magnetic fields to investigate the influence of Co substitutions on superconductivity, magnetism, and the interplay between both phenomena in the system $R(Ni_{1-x}Co_x)_2B_2C$ (R = Lu, Tm, Er, Ho, and Dy). Our results reveal that the superconducting transition temperature T_c decreases rapidly with increasing Co content for all rare-earth compounds. This decrease can be attributed to a decrease in the DOS at the Fermi level and is accompanied by a transition from clean to dirty limit behavior, as shown for $Lu(Ni_{1-x}Co_x)_2B_2C$. The rate of initial decrease dT_c/dx is lowest for the nonmagnetic system $Lu(Ni_{1-x}Co_x)_2B_2C$ and grows in magnitude from the Lu to the Ho compound. For $Ho(Ni_{1-x}Co_x)_2B_2C$ reentrant behavior is enhanced with increasing Co content. For the compounds $R(Ni_{1-x}Co_x)_2B_2C$ (R = Tm, Er) we observed the occurrence of reentrantlike behavior when the decreasing T_c comes close to the magnetic transition temperatures. For samples where T_c is below T_N, coexistence of superconductivity and magnetic order is observed again for all magnetic rare-earth compounds.

ACKNOWLEDGMENTS

We would like to thank W. Weber for fruitful discussions and his encouragement to extend our Co substitutions to all R compounds in the RNi_2B_2C series, and U. Gasser and P. Allenspach for discussing their work prior to publication. We also gratefully acknowledge the assistance in sample preparation of A. Krause and the technical support of W. Ettig.

[1] R. Nagarajan, C. Mazumdar, Z. Hossain, S.K. Dhar, K.V. Gopalakrishnan, L.C. Gupta, C. Godart, B.D. Padalia, and R. Vijayaraghavan, Phys. Rev. Lett. **72**, 274 (1994).

[2] R.J. Cava, H. Takagi, B. Batlogg, H.W. Zandbergen, J.J. Krajewski, W.F. Peck, Jr., T. Siegrist, K. Mizuhashi, J.O. Lee, H. Eisaki, and S. Uchida, Nature (London) **367**, 252 (1994).

[3] H. Eisaki, H. Takagi, R.J. Cava, K. Mizuhashi, J.O. Lee, B. Batlogg, J.J. Krajewski, W.F. Peck, Jr., and S. Uchida, Phys. Rev. B **50**, 647 (1994).

[4] J.L. Sarrao, M.C. de Andrade, J. Herrman, S.H. Han, Z. Fisk, M.B. Maple, and R.J. Cava, Physica C **229**, 65 (1994).

[5] H.C. Ku, C.C. Lai, Y.B. You, J.H. Shieh, and W.Y. Guan, Phys. Rev. B **50**, 351 (1994).

[6] C.C. Lai, M.S. Lin, Y.B. You, and H.C. Ku, Phys. Rev. B **51**, 420 (1995).

[7] C.V. Tomy, G. Balakrishnan, and D.McK. Paul, Physica C **248**, 349 (1995).

[8] B.K. Cho, P.C. Canfield, and D.C. Johnston, Phys. Rev. B **52**, R3844 (1995).

[9] T. Siegrist, H.W. Zandbergen, R.J. Cava, J.J. Krajewski, and W.F. Peck, Jr., Nature (London) **367**, 254 (1994).

[10] L.F. Mattheiss, Phys. Rev. B **49**, 3702 (1994).

[11] W.E. Pickett and D.J. Singh, Phys. Rev. Lett. **72**, 3702 (1994).

[12] R. Coehoorn, Physica C **228**, 331 (1994).

[13] M.S. Golden, M. Knupfer, M. Kielwein, M. Buchgeister, J. Fink, D. Teehan, W.E. Pickett, and D.J. Singh, Europhys. Lett. **28**, 369 (1994).

[14] A. Fujimori, K. Kobayashi, T. Mizokawa, K. Mamiya, A. Sekiyama, H. Eisaki, T. Takagi, S. Uchida, R.J. Cava, J.J. Krajewski, and W.F. Peck, Jr., Phys. Rev. B **50**, 9660 (1994).

[15] L.F. Mattheiss, T. Siegrist, and R.J. Cava, Solid State Commun. **91**, 587 (1994).

[16] S.K. Sinha, J.W. Lynn, T.E. Grigereit, Z. Hossain, L.C. Gupta, R.

Nagarajan, and C. Godart, Phys. Rev. B **51**, 861 (1995).
[17] J. Zarestky, C. Stassis, A.I. Goldman, P.C. Canfield, P. Dervenagas, B.K. Cho, and D.C. Johnston, Phys. Rev. B **51**, 678 (1995).
[18] B.K. Cho, P.C. Canfield, L.L. Miller, and D.C. Johnston, Phys. Rev. B **52**, 3684 (1995).
[19] R. Movshovich, M.F. Hundley, J.D. Thomson, P.C. Canfield, B.K. Cho, and A.V. Chubukov, Physica C **227**, 381 (1994).
[20] L.J. Chang, C.V. Tomy, D.McK. Paul, and C. Ritter, Phys. Rev. B **54**, 9031 (1996).
[21] P. Dervenagas, J. Zarestky, C. Stassis, A.I. Goldman, P.C. Canfield, and B.K. Cho, Physica B **212**, 1 (1995).
[22] H. Schmidt and H.F. Braun, Physica C **229**, 315 (1994).
[23] T.E. Grigereit, J.W. Lynn, Q. Huang, A. Santoro, R.J. Cava, J.J. Krajewski, and W.F. Peck, Jr., Phys. Rev. Lett. **73**, 2756 (1994).
[24] A.I. Goldman, C. Stassis, P.C. Canfield, J. Zarestky, P. Devenagas, B.K. Cho, and D.C. Johnston, Phys. Rev. B **50**, 9668 (1994).
[25] P. Dervenagas, J. Zarestky, C. Stassis, A.I. Goldman, P.C. Canfield, and B.K. Cho, Phys. Rev. B **53**, 8506 (1996).
[26] C. Detlefs, A.I. Goldman, C. Stassis, P.C. Canfield, and B.K. Cho, Phys. Rev. B **53**, 6355 (1996).
[27] J.Y. Rhee, X. Wang, and B.M. Harmon, Phys. Rev. B **51**, 15 585 (1995).
[28] H. Schmidt, M. Müller, and H.F. Braun, Physica C **235-240**, 779 (1994).
[29] A.K. Gangopadhyay, A.J. Schuetz, and J.S. Schilling, Physica C **243**, 317 (1995).
[30] S.L. Budko, M. Elmassalami, M.B. Fontes, J. Mondragon, W. Vanoni, B. Giordanengo, and E.M. Baggio-Saitovitch, Physica C **243**, 183 (1995).
[31] S.L. Budko, G.B. Demishev, M.B. Fontes, and E.M. Baggio-Saitovitch, J. Phys. Condens. Matter **8**, L159 (1996).
[32] C.C. Hoellwarth, P. Klavins, and R.N. Shelton, Phys. Rev. B **53**, 2579 (1996).
[33] P.B. Allen and R.C. Dynes, Phys. Rev. B **12**, 905 (1975).
[34] H. Michor, T. Holubar, C. Dusek, and G. Hilscher, Phys. Rev. B **52**, 1 (1995).
[35] T.P. Orlando, E.J. McNiff, Jr, S. Foner, and M.R. Beasley, Phys. Rev. B **19**, 4545 (1979).
[36] E. Helfand and N.R. Werthamer, Phys. Rev. **147**, 288 (1966).
[37] See, e.g., M. Decroux and Ø. Fischer, *Superconductivity in Ternary Compounds II*, edited by M.B. Maple and Ø. Fischer (Springer-Verlag, Berlin, 1982).
[38] W. Weber (unpublished).
[39] L.F. Rybaltchenko, I.K. Yanson, A.G.M. Jansen, P. Mandal, P. Wyder, C.V. Tomy, and D.McK. Paul, Europhys. Lett. **33**, 483 (1996).
[40] H. Schmidt, M. Weber, and H.F. Braun, Physica C **246**, 177 (1995).
[41] H. Schmidt, M. Weber, and H.F. Braun, Physica C **256**, 393 (1996).
[42] H. Schmidt and H.F. Braun (unpublished).
[43] P.C. Canfield, S.K. Budko, and B.K. Cho, Physica C **262**, 249 (1996).
[44] J.W. Lynn, Q. Huang, A. Santoro, R.J. Cava, J.J. Krajewski, and W.F. Peck, Jr., Phys. Rev. B **53**, 802 (1996).
[45] U. Gasser, P. Allenspach, and A. Furrer (unpublished).